Generating Efficient Behaviour with Predictive Visibility Risk for Scenarios with Occlusions

Lingguang Wang[1], Carlos Fernandez Lopez[1] and Christoph Stiller[1]

***Abstract*— Safety is one of the most significant challenges for autonomous driving. However, autonomous vehicles need also to be as efficient as possible while ensuring safety. In this paper we present an approach that helps the vehicle to drive efficiently in scenarios with occlusions, while being safe and comfortable. We quantify the visibility risk (VR) representing the collision risk with possible hidden obstacles in occlusions and anticipate the predictive VR by forecasting the scene in the short-term. The predictive VR can be integrated into the cost functional of arbitrary cost-based planning approach. By doing this, the vehicle is motivated to maintain a better view on the Region of Interest (ROI) on the map, which further opens up the scope of available behaviours and thus pursuing more efficient behaviour becomes possible. The proposed method is evaluated with a proof-of-concept planner decomposed into lateral (e.g. paths) and longitudinal directions (e.g. accelerations) in one overtaking scenario on a curved two-way street with dynamic occlusions and one intersection scenario with static occlusion, which shows promising results in vehicle driving efficiency.**

I. INTRODUCTION

Autonomous driving has been the focus of research for a long time. In the last years, large improvements have been made in perception and scene understanding. However, due to the limitation of sensor capability and the complex interaction between vehicle and environment, vehicle's sensing field might be limited either by the maximum sensing range or by surrounding obstacles. As the existence and states of the objects in the occluded area are unclear, it is more difficult for autonomous systems to balance safety, comfort and efficiency of the vehicle considering all possible events.

Safety has always the highest priority for fully automated vehicles. For this reason, the first challenge is to have reasonable prediction of surrounding traffic participants. Some previous work, such as [1] and [2] try to solve it in a probabilistic manner, but safety is difficult to guarantee. One promising approach is to compute reachable sets of the obstacles [3]. Safety is guaranteed as long as the trajectory of the ego vehicle does not intersect with those reachable sets. To tackle the possible hidden obstacles in occlusions, [4] over-approximates all possible states in the occluded areas. A combination of [3] and [4] could provide safety but a conservative behaviour would limit comfort and vehicle driving efficiency to some extent.

*This work is accomplished within the project "UNICARagil" (FKZ 16EMO0287) and the financial support from the Federal Ministry of Education and Research of Germany (BMBF) is acknowledged.

[1]Lingguang Wang, Carlos Fernandez Lopez and Christoph Stiller are with the Institute of Measurement and Control Systems, Karlsruhe Institute of Technology (KIT), Karlsruhe, Germany lingguang.wang, carlos.fernandez, stiller@kit.edu

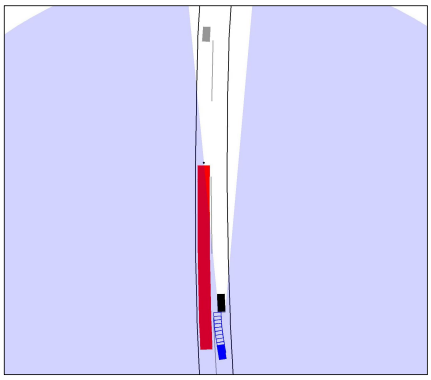

Fig. 1: Ego vehicle (blue box) intends to overtake the slow-moving car ahead (black box) on a two-way road with oncoming vehicle (gray box), which is occluded by the black vehicle. Thus, the overtaking is dangerous because of the reachable set (red polygon) of possible hidden obstacles.

In the scenario depicted in Fig. 1, it is dangerous for the ego vehicle to overtake the slow-moving vehicle ahead due to possible obstacles that could emerge from occlusions. In this case, human drivers will first move closer to the dashed centerline to obtain more information about the oncoming lane. Humans will only overtake after confirm that there is enough space on the opposite lane. Before that, they have already considered the possible oncoming vehicles in the occlusion implicitly. Thus, they act cautiously to try to improve their visibility beforehand.

From this example we speculate that in some scenarios with occlusions, an active increase of visibility can produce more efficient behaviours, which were verified as unsafe before. For obtaining this human-like behaviour, we propose the predictive VR and integrate it into a proof-of-concept behaviour planner. By doing so, the vehicle is able to select an action that brings more potential future visibility on the ROI, does not collide with visible and invisible obstacles and is optimal in the sense of comfort and efficiency.

The rest of the paper is organized as follows: Section II discusses the related work. In Section III we introduce some preliminaries. The predictive VR is then described in Section IV. In Section V, we evaluate the approach in some scenarios in simulation and the results are presented. Finally, we conclude this paper and discuss the future work in Section VI.

II. RELATED WORK

The goal of this paper is to provide more efficient decisions in the scenarios with occlusions while maintaining

safety and comfort. However, previous work was mainly focus either only on safety, or only on efficiency without safety proof.

As already introduced, [4] assumes worst-case scenarios for all possible obstacles inside the invisible area to provide provable safety but less comfort plan, while others ([5] and [6]) consider uncertainties to solve the comfort issue but give less safety guarantees. [7] does probabilistic risk assessment of unobservable regions and utilizes an optimization-based motion planner to reduce the collision rate while still maintaining certain comfort level, but safety is not guaranteed. [8] puts probabilistic consideration into prediction of objects being at the edge of the field of view, thus to get safe but not overcautious reaction compared to [4]. However, it does not enable the vehicle to actively reduce the risk caused by visibility loss and thus miss the opportunity to improve efficiency.

Recently [9] takes future field of view (FoV) into account by formulating the planning problem as Partially Observable Markov Decision Process (POMDP). This is a promising approach regarding future FoV maximization. However it is not able to provide any guarantee on safety and solving POMDP is also computationally intractable. [10] models the visibility maximization as a non-linear constrained optimization problem, and shows the effectiveness on overtaking static obstacles, yet it lacks evaluation on overtaking moving obstacles in unstructured environment. Another problem is that maximizing view angle alone won't work for generic road topologies where only certain parts of the road are interesting for the current behaviour planning.

Therefore, our contributions compared with previous work are the following:

- We quantify predictive VR associated with the predicted FoV and the ROI (explained in Section IV-A), which is planning algorithm agnostic and enables us to adopt more efficient and comfortable behaviours.
- Our approach can ensure provable Responsibility-Sensitive Safety (RSS) [11] while performing more efficient behaviours, such as safe overtaking instead of following slow-moving obstacles and traversing an unsignalized intersection with occlusions faster.
- Our approach works with arbitrary road topologies.

III. PRELIMINARIES

In this section, we first explain the proof-of-concept trajectory planner in III-A that we used for evaluation. Then in III-B we generate predictions for visible obstacles and possible hidden obstacles in occlusions. These predictions will be used for collision check in the subsequent section.

A. Trajectory Planner

We employ path-velocity decomposition for the planner. In lateral direction, we generate several path candidates $\mathcal{T} = \{\tau_1, \tau_2, \ldots, \tau_N\}$ with different lateral offsets in Frenét frame [12] using cubic polynomial [13], which allows easier handling of the road curvature, as Fig. 2 shows.

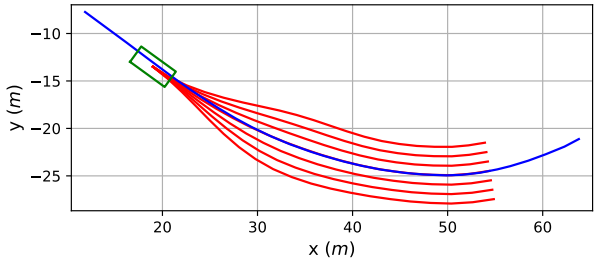

Fig. 2: Generated local path candidates (red) with respect to the centerline (blue).

On each path, the longitudinal action will be divided into two parts, e.g. following one acceleration for the first 1.6 seconds (common reaction time of an experienced autonomous driving system [14]) and applying full brake ($-4m/s^2$) for the remaining planning horizon. The acceleration is selected from the candidate accelerations $\mathcal{A} = \{a_1, a_2, \ldots, a_M\}$. We discretize the planning horizon into K time steps with time interval Δt.

At each planning step, one path τ_j and its corresponding optimal acceleration a_i will be chosen as the action (a_i, τ_j), which guides the ego vehicle until the next planning step. The action space S_a is the set of all possible candidate actions:

$$S_a = \{A_{i,j}\}, \text{ with } A_{i,j} = (a_i, \tau_j), \ for\ a_i \in \mathcal{A}, \tau_j \in \mathcal{T} \tag{1}$$

B. Reachable Set Prediction

As already explained in previous sections, a reachability-set based prediction will be utilized for the obstacles to ensure provable active safety. As long as other traffic participants follow traffic rules and the ego vehicle trajectory does not fall into the reachable sets of others, the active safety is guaranteed despite negligible control errors. We model road geometry and topology based on lanelet2 map [15]. Obstacle reachable sets with known initial states at time step n can be represented by occupancy polygons. To perform a lane-following reachable set based prediction of a vehicle, assumptions such as the maximum velocity v_{max} (e.g. 110% of the speed limit), acceleration a_{max}, deceleration a_{min} and prohibiting driving backwards will be made at first. Then longitudinal starting and end boundaries s_{min} and s_{max} of the occupancy polygon on the Frenét frame with respect to the corresponding centerline can be computed as in (2) and (3). Fig. 3(a) shows a qualitative example.

$$s_{max}(n) = \begin{cases} v_0 t + \frac{1}{2} a_{max} (t)^2 & (v_0 + t a_{max} \leq v_{max}) \\ v_{max} t - \frac{(v_{max} - v_0)^2}{2 a_{max}} & (v_0 + t a_{max} > v_{max}) \end{cases} \tag{2}$$

$$s_{min}(n) = \begin{cases} \frac{1}{2}(2 v_0 + a_{min} t) t & (v_0 + t a_{min} \geq 0) \\ -\frac{v_0^2}{2 a_{min}} & (v_0 + t a_{min} < 0) \end{cases}, \quad t = n \Delta t, n \in \{0, \ldots, K\} \tag{3}$$

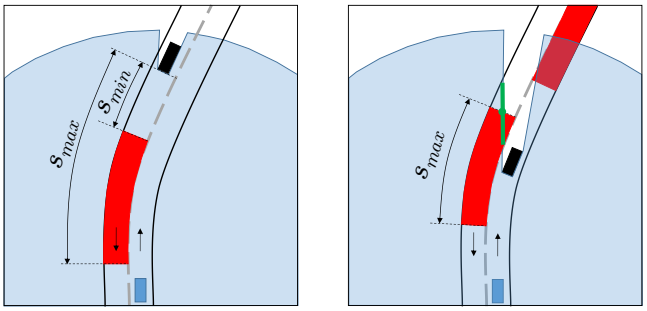

(a) (b)

Fig. 3: Occupancy polygons of the visible obstacles and the critical sensing edge under the current FoV (translucent blue polygon). (a) Reachable occupancy polygon (red polygon) of the visible obstacle (black box) on the oncoming lane. (b) Over-approximated occupancy polygon (left red polygon) of the critical sensing edge (green segment).

As shown in Fig. 3, FoV is modelled as a polygon. The polygon may intersect with the lanelets, and result in several critical sensing edges (CSE), from which obstacles with arbitrary initial states (e.g. velocity, position and orientation) could appear. The reachable sets for these possible hidden obstacles can be represented as occupancy polygons as well. However, their initial states should be over-approximated [4]. In this case, s_{min} should be 0 at all time steps, because there could be obstacles appearing just at the CSE at any time. We select CSE centre as the starting point of the occupancy polygon. Maximum velocity v_{max} is used to compute the end boundary of the occupancy polygon at each time step. Thus, the s_{max} is simply $v_{max} n \Delta t$, as Fig. 3(b) illustrates.

The lateral bounds of the occupancy polygon will be left and right lane boundaries, which differs from the original concept in [3], with the consideration that lane change behaviours of the obstacles in the evaluated scenarios are either illegal or unnecessary.

IV. RISK-MINIMIZING BEHAVIOUR PLANNING

The behaviour planning output is the optimal action $A_{i,j}$ from the action space S_a in the sense of minimum cost. To encourage the vehicle to select the path which could bring more future visibility on the ROI, we introduce the predictive VR, which will be explained in Section IV-A, inspired by [16]. Furthermore, by adding the predictive VR into the cost functional that already balances comfort and utility and weighting them properly, the desired behaviour of active exploration on invisible areas can be obtained (Section IV-B).

A. Predictive Visibility Risk

It is assumed that all the static and dynamic obstacles are detected and tracked by the perception module and thus their states are known as prior. Based on this, several definitions are firstly made before introducing the concept.

Definition 1 (Region of Interest, ROI). *The area, on which the traffic participants have priority or right of way under the current location, intention and sensing capability of the ego vehicle.*

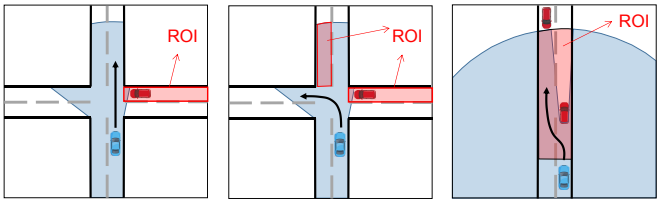

(a) (b) (c)

Fig. 4: ROI (red polygons) and FoV (blue polygons). (a) Ego vehicle (blue vehicle) intends to go straight at an unsignalized intersection. (b) Ego vehicle tends to turn left. (c) Overtaking on a two-way street.

Ensuring absolute safety on the road is impossible [11]. However, as long as we don't take priority from the traffic participants on the ROI and don't crush into them, RSS is guaranteed. The ROI is dynamic as the ego vehicle is changing its location. It can be theoretically unlimited, e.g. due to an extremely long priority lane, which is not possible for calculation. Thus, we restrict it by the maximum sensing range of the ego vehicle. It also depends on the current driving intention. For example, when approaching an unsignalized junction, the ego vehicle can have two possible intentions: 1) going straight, the ROI is only the road coming from the right side where the vehicles have the right of way (Fig. 4(a)). 2) turning left, the ROI should additionally include the area on the oncoming lane (Fig. 4(b)). In an overtaking scenario, e.g. in Fig. 3, the ROI is the area in front of the ego vehicle on both lanes (Fig. 4(c)). Thus, ROI could also be plural. Given the global route and the local intended behaviour of the ego vehicle, the ROIs can be easily extracted with the HD Map frameworks, e.g. lanelet2 [15].

Definition 2 (Occlusion Critical Obstacles, OCO). *All the static and dynamic obstacles that block the visibility of the ego vehicle on the ROIs at least partially.*

Definition 3 (Single-shot state). *The state (global position, velocity, dimension) of the ego vehicle S_{ego} and the states of all the OCO S_{oco}.*

1) Single-Shot Visibility Risk: We first define the VR for one single-shot state. Imaging that the ego vehicle faces some loss of FoV on the ROIs before entering one intersection or performing overtaking, it would feel a certain level of risk depending on how much the collision probability with the possible hidden obstacles on the invisible ROIs is and how critical the collision might be.

In order to first approximate the collision probability, we sample N_p particles on the ROIs, each of them simulates one obstacle pursuing the lane with certain velocity. Their velocities and x-coordinates in Frenét frame are sampled from uniform distributions $v \sim U([v_{min}, v_{max}])$ and $x \sim U([x_{min} + 0.5l, x_{max} - 0.5l])$, where v_{min} and v_{max} denote the minimum and maximum velocity of the particles. x_{min} and x_{max} are the starting and ending position of the centerline segment cut by the ROI. l is the length of the obstacle. To model the lateral displacement, an offset y is

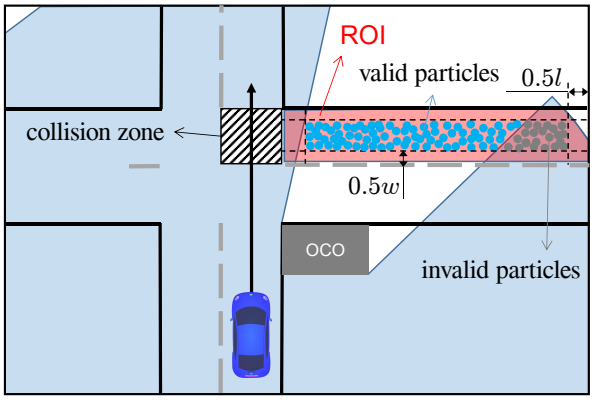

Fig. 5: Generated valid (blue) and invalid particles (gray).

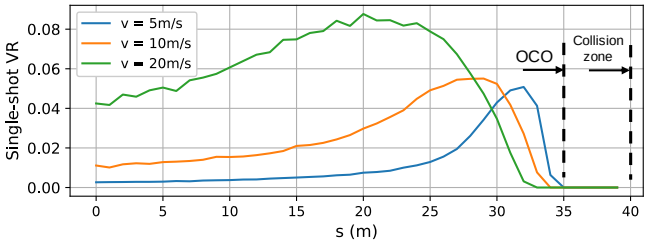

Fig. 6: Single-shot VR changes with travelled distance while passing the intersection with different velocity in scenario of Fig. 5.

sampled from $y \sim U([-d(x) + 0.5w,\ d(x) - 0.5w])$, where $d(x)$ is the lane width at the x-coordinate x in Frenét frame, and w is the obstacle width. There are two things to note: 1) Only the particles in the invisible ROIs will be treated as *valid particles*, and the other particles are *invalid particles* that will be abandoned directly. 2) The invisible ROIs should not contain particle if the length of its centerline segment is shorter as l. Fig. 5 depicts one example where the ego vehicle intends to go straight at one unsignalized intersection.

For each ROI, one collision zone is specified. For example, the number of collision zones associated with the ROIs for the scenario in Fig. 4(b) will be two. Assuming that the ego vehicle moves with the current velocity following the intended path, and the sampled valid particles follow the lane with the initialized velocity while maintaining the original lateral offsets, the particles will be critical if they will collide with ego vehicle on the corresponding collision zone. We call those critical particles (CP). Obviously, the collision probability P_i will be 1 if i-th particle belongs to CP, otherwise 0.

To estimate the severity of the collision with i-th particle S_i, we utilize square of relative velocity ${v_r^i}^2$ and normalize it to 1 with the square of maximum possible relative velocity $v_{r,max}^2$. Thus, $S_i = (\frac{v_r^i}{v_{r,max}})^2$.

Hence, as a function of S_{ego} given the states of the OCO S_{oco}, the single-shot VR R_s can be defined as the average collision risk over all the N_p sampled particles (including valid and invalid particles), as in (4)

$$R_{s,S_{oco}}(S_{ego}) = \frac{1}{N_p}\sum_{i=1}^{N_p} P_i S_i \tag{4}$$

We simulate the scenario in Fig. 5 with vehicle passing through the intersection at different velocity, and observe how the single-shot VR changes with the travelled distance and velocity, jet with no real obstacles in the occlusion. As depicted in Fig. 6, the single-shot VR has the following properties: 1) driving slowly, it is low overall due to lower severity, apart from when the vehicle is close to the OCO, where collisions with more particles occur. 2) driving fast, it will be high overall, except when the vehicle is close to the OCO, due to the fact that the vehicle is able to pass the collision zone faster than most of the particles as it can already see far enough. There are two other properties that can be easily asserted: the single-shot VR will be low 3) if the distance between the invisible ROI to the collision zone is large such that all the valid articles are far away from the collision zone, or 4) if the area of the invisible ROI is small compared to the area of the ROI because a lot of particles are treated as invalid particles and will not be counted as CP.

All these properties match how human driver perceives VR. In order to minimize it, the vehicle should either adjust the speed depending on how close it is to OCO, or enlarge the visible area on ROIs. However, we could not simply infer from single-shot VR, where to move to achieve the latter.

2) Predictive Visibility Risk: To incentivize vehicles to control speed and select paths in the direction of reducing future VR, we also estimate the predictive VR associated with the chosen action.

There are basically three factors that influence how the visibility on the ROIs changes in the short future: 1) which path it follows. 2) how the OCO move. 3) how fast the ego vehicle drives. The first and third conditions depend on which action (a, τ) the ego vehicle selects. The second condition can only be coarsely estimated due to the obscurity of OCO's future movement. However, we could simply adopt constant velocity for the OCO, since what we want is only a rough "guess" on which path could provide a better future visibility and it has nothing to do with safety. For instance, one static OCO (with velocity 0) should be expected to continue being static, because we don't expect that it suddenly actively moves away to give us a better view. The horizon chosen for estimating the visibility gain or loss in the short future should not be as long as the whole planning horizon, because a long-term estimation is neither accurate nor necessary.

We formulate the predictive VR as the weighted sum of the single-shot VR for X planning steps, which is a function of the chosen action (a, τ), given the constant velocity motion estimation of the OCO $S_{oco}(t)$.

$$R(a,\tau) = \sum_{x=0}^{X} \gamma^x R_{s,S_{oco}(x\Delta t)}(S_{ego}(x\Delta t, a, \tau)) \tag{5}$$

Note that there are factors that may lead to inaccurate predictive VR, e.g. hidden obstacles that may cause unexpected

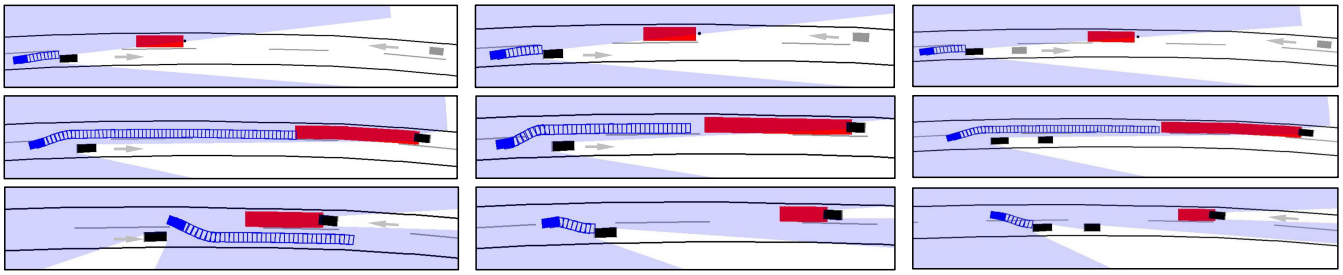

(a) Top view for time 0s, 2s and 6s (b) Top view for time 0s, 2s and 4s (c) Top view for time 0s, 2s and 8s

Fig. 7: Overtaking scenarios on a two-way street with oncoming traffic. The reachable sets of obstacles in ego lane are not rendered. Different prediction horizon for overtaking yields longer length of the occupancy polygon in the middle figures as the left and right one. (a) Ego vehicle overtakes the slow-moving obstacle safely. (b) Ego vehicle tries to overtake but abort the manoeuvrer due to too close oncoming obstacle. (c) Ego vehicle abort the overtaking due to invisible second obstacle on the ego lane.

future occlusion and imperfection of the motion estimation of OCO. To facilitate this, $\gamma \in [0, 1]$ is introduced as a discount factor which adjusts our trust on the estimated future FoV. The bigger the γ, the more we believe in our estimation about the short future.

B. Cost Formulation

In order to get a comfortable, safe and efficient behaviour, we need to iterate through all possible combinations of action (a, τ) with $a \in \mathcal{A}$ and $\tau \in \mathcal{T}$ and select the action which balances all the objectives appear in the cost functional.

For a comfortable behaviour, we minimize the square of the acceleration. To prevent big acceleration jump between two time steps that a real car can't follow, we penalize acceleration changes $a - a_l$ as well, where a_l denotes the selected acceleration at last planning step.

Regarding safety, the actions and their corresponding trajectories, which intersect with the predicted occupancy polygons, will be discarded. This will reduce the available action space S_a to safe action space $S_{a,safe}$, which ensures provable safety under the aforementioned assumptions. If all the candidate actions are not safe, the trajectory which was computed at the last planning step and was verified as safe, will be served as fallback and followed till the end.

The desired velocity $v_{desired}$ is introduced for maximizing utility. The ego vehicle try to reach $v_{desired}$ by adapting its acceleration according to the deviation of the current velocity $v_{current}$ from $v_{desired}$, i.e. the expected acceleration will be proportional to the deviation of $v_{current}$ from $v_{desired}$.

For more realistic behaviour, we penalize the deviation of the path τ from the centerline τ_c and from the last selected path τ_l as in (6)

$$DC(\tau) = (d(\tau))^2, DL(\tau) = (d(\tau) - d(\tau_l))^2 \tag{6}$$

where $DC(\tau)$ and $DL(\tau)$ are the cost terms. $d(\tau)$ denotes the lateral offset of the path τ from centerline τ_c. Finally, the cost functional can be formulated as in (7)

$$\begin{aligned} J(A_{i,j}) =& w_1 R(A_{i,j}) + w_2 a_i^2 + w_3 (a_i - a_l)^2 + \\ & w_4 (1 - k\frac{a_i}{a_{max}} - \frac{v_{current}}{v_{desired}})^2 + \\ & w_5 DC(\tau_i) + w_6 DL(\tau_i),\ A_{i,j} \in S_{a,safe} \end{aligned} \tag{7}$$

where w_1, w_2, w_3, w_4, w_5, w_6 and k are parameters that are manually fine-tuned. Note that we only use a_{max} as the reference acceleration for accelerating and decelerating because we choose $a_{min} = -a_{max}$ in Section V. The optimal action A^* can be determined by

$$A^* = \underset{A_{i,j} \in S_{a,safe}}{\arg\min}\ J(A_{i,j}) = \underset{A_{i,j} \in S_{a,safe}}{\arg\min}\ J((a_i, \tau_j)) \tag{8}$$

V. RESULTS

We evaluated our method on two typical streets in simulation where occlusion plays a significant role. One is overtaking on a curved two-way street with dynamic occlusion related obstacles, see Fig. 7.

The other one is an intersection under occlusion, which is mapped from a real intersection in the city of Karlsruhe, see Fig. 8. Our method shows promising results in maintaining desired velocity by actively exploring the invisible ROI while keeping safe and comfort.

A perfect perception of obstacles is assumed from a 360-degree range sensor mounted on the top centre of the vehicle. For overtaking on the test street with a speed limit of $50km/h$, $200m$ sensing range is assumed, while for the intersection with a speed limit of $30km/h$, $50m$ is enough, thus $v_{max} = v_{desired} = 1.1 v_{limit}$ are $15m/s$ and $10m/s$ for these two scenarios respectively. $\mathcal{A}$ is chosen to be $\{-4m/s^2, -3.9m/s^2, \ldots, 4m/s^2\}$. Other parameters are listed in Table I.

TABLE I: Chosen parameters for the evaluation.

v_{min} (m/s)	l (m)	w (m)	$v_{r,max}$ (m/s)	N_p	X	Δt (s)	K	γ
0.0	5.0	2.5	30.0	50000	10	0.1	50	0.8

A. Overtaking on a Two-way Street with Dynamic OCO

We select 3 lateral offsets for generating the path candidates $\mathcal{T} = \{\tau_{overtake}, \tau_{approach}, \tau_c\}$. $\tau_{overtake}$ is the overtaking path which leads the ego vehicle to the opposite lane. $\tau_{approach}$ is the path that leads the ego vehicle to the left border of the ego lane and thus to approach the centre of the street to have a better view on the opposite lane.

In the test scenarios, the obstacles in the ego lane are moving with $6m/s$. Given the fact that in reality, those slow-moving obstacles (e.g. agricultural machine) don't have much potential for accelerating and decelerating, their a_{max} and a_{min} are set to $1m/s^2$ and $-1m/s^2$ for prediction.

In order to guarantee a safe overtake and a safe follow driving, different prediction horizons are employed for different path candidates as pointed out in [17]. For $\tau_{overtake}$, the time that needed to finish the overtaking is used and thus to avoid collision with oncoming obstacle. This can be estimated by assuming that the ego vehicle accelerates with a medium acceleration $2m/s^2$, and the furthest obstacle that we can see and want to overtake accelerates with its $a_{max} = 1m/s^2$. For $\tau_{approach}$ and τ_c, we utilize the time-to-stop as the prediction horizon, which ensures that the ego vehicle can come to a full stop within the prediction horizon.

We set three distinct overtaking scenarios. The first one is overtaking one slow-moving obstacle in the ego lane, with an oncoming obstacle (velocity $6m/s$) far away, corresponding to Fig. 7(a). The ego vehicle tries first to follow $\tau_{approach}$ to increase the visibility. After having far enough FoV on the opposite lane, it switches to $\tau_{overtake}$ and finally accomplish the overtaking successfully. The second scenario shown in Fig. 7(b) is similar to the first one except that the oncoming obstacle is closer. After a short attempt to overtake, it is forced to abort its overtaking manoeuvrer and switches back to $\tau_{approach}$. The third scenario depicted in Fig. 7(c) is also similar to Fig. 7(a), but has two obstacles in the ego lane. After discovering the second obstacle which wasn't visible before, the ego vehicle gives up overtaking because the time-to-overtake increases a lot.

Without integrating predictive VR, the ego vehicle will not be motivated to choose $\tau_{approach}$ because it has higher cost due to deviation from the centerline. Meanwhile, it can never start overtaking because the opposite lane is always occupied by the reachable sets of the critical sensing edge.

B. Crossing Intersection with Static OCO

In this scenario, we select five offsets for $\mathcal{T}$ inside the ego lane and use time-to-stop as the prediction horizon. One static obstacle (e.g. a parked car) occludes the right arm of the intersection. We compared our approach with the baseline approach [4], which didn't take predictive VR into account.

As can be seen in Fig. 8(b), using our approach, the vehicle tends to move to the left side and brake earlier when approaching the intersection, which imitates how human drivers maximize the FoV and reduce the VR. Thanks to this behaviour, the ego vehicle shows following advantages over the baseline (Fig. 8(a)), while still ensuring provable safety: it 1) approaches the intersection with a smaller deceleration and is thus more comfortable, 2) maintains a higher average speed and thus more efficient, 3) is less risky with respect to potential collision with possible hidden obstacles, as Fig. 8(c) depicts.

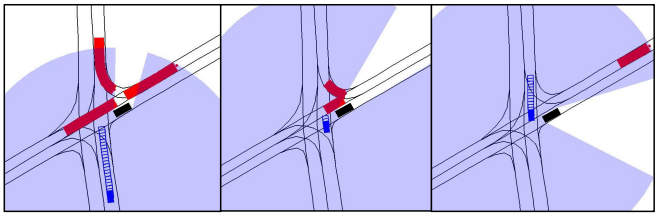

(a) Top view for time 0.5s, 4.4s and 5.6s

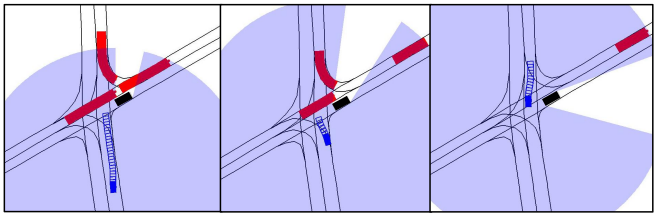

(b) Top view for time 0.3s, 4s and 5.4s

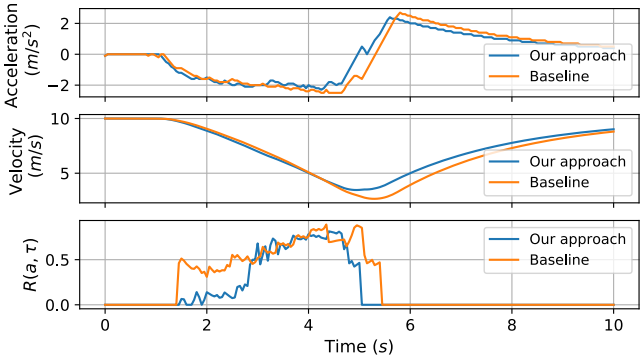

(c)

Fig. 8: Crossing an intersection with static OCO. (a) Baseline approach. (b) Taking the predictive VR into account and imposing it into the cost functional. (c) Comparison of their predictive VR $R(a, \tau)$.

VI. CONCLUSIONS AND FUTURE WORK

The paper introduces the predictive VR in order to provide not overly conservative driving behaviour but guarantee safety. This is done by incorporating active exploration in a sense that the ego vehicle would make moves to gain visibility. The proposed method has proven its effectiveness in performing overtaking on a curved two-way street and passing unsignalized intersection with occlusions more efficiently as the baseline model, while being safe and comfort.

However, our approach is not only limited to autonomous vehicles. Building a risk monitoring system on top of that for driving assistance is also sufficient. It can further be applied for navigating robots more efficiently in highly unstructured environments under occlusions, e.g. by switching the underlying trajectory planner to different algorithms, such as RRT in [18] or graph search-based path planning [19], and sampling particles to represent all possible hidden obstacles (pedestrians, bicycles, etc.).

Another potential improvement on efficiency will be tracking the occlusion with particles, which could reduce the initial state intervals of hidden obstacles significantly. However, dealing with memory of previous scenes needs delicate design of the tracker, and the safety is again hard to guarantee since the sampled particles can hardly cover all the possibilities in occlusion.

REFERENCES

[1] J. Wiest, M. Hffken, U. Kreel, and K. Dietmayer, "Probabilistic trajectory prediction with gaussian mixture models," in *2012 IEEE Intelligent Vehicles Symposium*, June 2012, pp. 141–146.

[2] B. Kim, C. M. Kang, S. Lee, H. Chae, J. Kim, C. C. Chung, and J. W. Choi, "Probabilistic vehicle trajectory prediction over occupancy grid map via recurrent neural network," *CoRR*, vol. abs/1704.07049, 2017. [Online]. Available: http://arxiv.org/abs/1704.07049

[3] M. Althoff and S. Magdici, "Set-based prediction of traffic participants on arbitrary road networks," *IEEE Transactions on Intelligent Vehicles*, vol. 1, no. 2, pp. 187–202, June 2016.

[4] P. F. Orzechowski, A. Meyer, and M. Lauer, "Tackling occlusions & limited sensor range with set-based safety verification," *CoRR*, vol. abs/1807.01262, 2018. [Online]. Available: http://arxiv.org/abs/1807.01262

[5] S. Hoermann, F. Kunz, D. Nuss, S. Renter, and K. Dietmayer, "Entering crossroads with blind corners. a safe strategy for autonomous vehicles," in *2017 IEEE Intelligent Vehicles Symposium (IV)*, June 2017, pp. 727–732.

[6] W. Zhan, C. Liu, C. Chan, and M. Tomizuka, "A non-conservatively defensive strategy for urban autonomous driving," in *2016 IEEE 19th International Conference on Intelligent Transportation Systems (ITSC)*, Nov 2016, pp. 459–464.

[7] M. Yu, R. Vasudevan, and M. Johnson-Roberson, "Occlusion-aware risk assessment for autonomous driving in urban environments," *CoRR*, vol. abs/1809.04629, 2018. [Online]. Available: http://arxiv.org/abs/1809.04629

[8] M. Naumann, H. Königshof, M. Lauer, and C. Stiller, "Safe but not overcautious motion planning under occlusions and limited sensor range," 2019.

[9] C. Hubmann, N. Quetschlich, J. Schulz, J. Bernhard, D. Althoff, and C. Stiller, "A pomdp maneuver planner for occlusions in urban scenarios," 06 2019.

[10] H. Andersen, W. Schwarting, F. Naser, Y. H. Eng, M. H. Ang, D. Rus, and J. Alonso-Mora, "Trajectory optimization for autonomous overtaking with visibility maximization," in *2017 IEEE 20th International Conference on Intelligent Transportation Systems (ITSC)*, Oct 2017, pp. 1–8.

[11] S. Shalev-Shwartz, S. Shammah, and A. Shashua, "On a formal model of safe and scalable self-driving cars," *CoRR*, vol. abs/1708.06374, 2017. [Online]. Available: http://arxiv.org/abs/1708.06374

[12] M. Werling, J. Ziegler, S. Kammel, and S. Thrun, "Optimal trajectory generation for dynamic street scenarios in a frenet frame," 06 2010, pp. 987 – 993.

[13] K. Chu, M. Lee, and M. Sunwoo, "Local path planning for off-road autonomous driving with avoidance of static obstacles," *IEEE Transactions on Intelligent Transportation Systems*, vol. 13, no. 4, pp. 1599–1616, Dec 2012.

[14] V. Dixit, S. Chand, and D. Nair, "Autonomous vehicles: Disengagements, accidents and reaction times," *PLOS ONE*, vol. 11, p. e0168054, 12 2016.

[15] F. Poggenhans, J.-H. Pauls, J. Janosovits, S. Orf, M. Naumann, F. Kuhnt, and M. Mayr, "Lanelet2: A high-definition map framework for the future of automated driving," 11 2018, pp. 1672–1679.

[16] X. Xiao, J. Dufek, and R. R. Murphy, "Explicit-risk-aware path planning with reward maximization," *CoRR*, vol. abs/1903.03187, 2019. [Online]. Available: http://arxiv.org/abs/1903.03187

[17] P. Orzechowski, K. Li, and M. Lauer, "Towards responsibility-sensitive safety of automated vehicles with reachable set analysis," 11 2019, pp. 1–6.

[18] S. Karaman and E. Frazzoli, "Sampling-based algorithms for optimal motion planning," *CoRR*, vol. abs/1105.1186, 2011. [Online]. Available: http://arxiv.org/abs/1105.1186

[19] S. Bhattacharya, V. Kumar, and M. Likhachev, "Search-based path planning with homotopy class constraints," in *Proceedings of the Twenty-Fourth AAAI Conference on Artificial Intelligence*, ser. AAAI'10. AAAI Press, 2010, pp. 1230–1237. [Online]. Available: http://dl.acm.org/citation.cfm?id=2898607.2898803